



1                                   **Geological Stratigraphy and Spatial Distribution of**  
2                                   **Microfractures over Costa Rica Convergent Margin, Central**  
3                                   **America- A Wavelet-Fractal Analysis**

4                                   Upendra K. Singh, Thinesh Kumar and Rahul Prajapati,  
5                                   Department of Applied Geophysics, Indian School of Mines, Dhanbad-826 004, India

6                                   Correspondence: [upendra\\_bhui@rediffmail.com](mailto:upendra_bhui@rediffmail.com)

7                                   **Abstract**

8                                   Identification of spatial variation of lithology, as a function of position and scale, is very  
9                                   critical job for lithology modelling in industry. Wavelet Transform (WT) is an efficacious  
10                                   and powerful mathematical tool for time (position) and frequency (scale) localization. It has  
11                                   numerous advantages over Fourier Transform (FT) to obtain frequency and time information  
12                                   of a signal. Initially Continuous Wavelet Transform (CWT) is applied on gamma ray logs of  
13                                   two different Well sites (Well-1039 & Well-1043) of Costa Rica Convergent Margin, Central  
14                                   America for identifications of lithofacies distribution and fracture zone later Discrete Wavelet  
15                                   Transform (DWT) applied to DPHI log signals to show its efficiency in discriminating small  
16                                   changes along the rock matrix irrespective of the instantaneous magnitude to represent the  
17                                   fracture contribution from the total porosity recorded. Further the data of the appropriate  
18                                   depths partitioned using above mathematical tools are utilized separately for WBFA. As  
19                                   consequences of CWT operation it is found that there are four major sedimentary layers  
20                                   terminated with a concordant igneous intrusion passing through both the wells. In addition of  
21                                   WBFA analysis, it is clearly understanding that the fractal dimension value is persistent in  
22                                   first sedimentary layers and the last gabbroic sill intrusions. Inconsistent value of fractal  
23                                   dimension is attributed to fracture dominant in intermediate sedimentary layers it is also  
24                                   validate through core analysis. Fractal Dimension values suggest that the sedimentary



25 environments persisting in that well locations bears abundant shale content and of low energy  
26 environments.

27 **Key words:** CWT, DWT, Fractal, Costa Rica.

28

## 29 **1. Introduction**

30 The nature of any log signal is fluctuating type in accordance to the subsurface geology. A  
31 gamma ray log is most vividly used log for lithology identifications. These signals are very  
32 noisy in some cases and highly fluctuating in another way. Manual interpretations of such  
33 signals are quite difficult and it needs more experience. These difficulties are minimised by  
34 kind of wavelet transform method. In our study Continuous Wavelet transform (CWT) is  
35 tested on generated synthetic signals and applied to field data. The analysed results prove that  
36 the CWT is highly suitable in geophysical log signals whereas conventional Fast Fourier  
37 Transform fails in this case because it considers the whole signal in a stationary form.  
38 Though Wavelet Transform provides unambiguous results in analysing the noisy and non-  
39 stationary signals, its efficiency of extracting the information from the signal was seen  
40 through its wavelet coefficients (Hui and Zaixing, 2010) with wavelet scalogram. Number of  
41 publication has come to identify the lithofacies/boundary using various mother Wavelet  
42 transform and Fourier transform (Chandrasekhar et al., 2012; Coconi et al., 2010; Dashtian,  
43 2011; Javid and Tokhmechi, Mansinha et al.,1997; Mansinha 2003, 2004; Pan et al.,2007,  
44 2012; Pinnegar and Stockwell, 2007; Stockwell et al., 1996; Sahimi and Hashemi, 2001;  
45 Tokhmechi et al., 2009a, b; Yue et al., 2004; Zhang et al., 2011;).

46

47 In this paper, CWT and Discrete wavelet transform (DWT) are used separately for identifying  
48 the lithology using gamma ray log data of well site 1039 and 1043 obtained from Costa Rica  
49 Convergent Margin, Central America and computed wavelet scalograms. Moreover, the



50 information of fractures zones is analyzed with DWT using density logs data for both wells  
51 that provides well featured whereas the log data doesn't carry information of fracture remains  
52 featureless. Afterward, a linear relationship is obtained between the fracture density obtained  
53 through DWT and identified fractures from water saturation logs using above methods. Apart  
54 from wavelet analysis, one of the approach wavelet based fractal analysis techniques applied  
55 to attribute the roughness/smoothness of the fractures. The obtained suggest that wavelet  
56 transform acts as a microscope to delineate the high and low frequency hidden in the signal  
57 separately, wavelet/holder exponent and fractal dimension are highly useful in identification  
58 of lithofacies and spatial distribution of fractures.

59

## 60 **2. Mathematical Background**

### 61 **2.1 Wavelet Transform**

62 Wavelet transform is mathematical tool that can be used to analyse both stationary and non-  
63 stationary signals (Daubechies 1990, 1992) and expand time series into time frequency space.  
64 Therefore, this method can find localized intermittent periodicities. For analysing stationary  
65 or non-stationary signal proper mother wavelet has to be substituted and the operation of  
66 continuous wavelet transform (CWT) proceeds as the convolution between time series of our  
67 interest. The Discrete wavelet transform (DWT) is very useful in case of noisy data it  
68 compresses the data by reducing noise and improve the resolution whereas the application of  
69 CWT is preferring to extract the lithological feature from data. As it exposes the signal to  
70 high and low frequency filters to form approximate and detailed coefficients traces out the  
71 abrupt changes in the signal (Figure 8a and 8b). Basically, in geophysical well logs the abrupt  
72 change corresponds to its own individual parameter changes which provide us more  
73 information about the subsurface stratigraphy. This methodology pertaining to DWT allows  
74 us to locate the high frequency changes immersed in the log which cannot be identified



75 manually. For example, gamma ray log is a good lithology indicator but in certain conditions  
76 it is highly fluctuating in nature. This nature sometimes perturbs its evaluation. Apart from  
77 lithology identification, DWT provides an advantage of analysing the fracture identifications.

78

## 79 **2.2Continuous Wavelet Transform**

80 The concept of continuous wavelet transform can be explained by a basic equation given  
81 below:

$$82 \quad W(a, b) = \frac{1}{a^n} \int_{-\infty}^{\infty} f(x) \varphi\left(\frac{x-b}{a}\right) dx \quad (1)$$

83 Where,  $f(t)$  is the time series of our interest;

84  $\varphi(t)$  is the mother wavelet;

85  $a$  is the scaling parameter otherwise denoted as the Inverse of Frequency;

86  $b$  is the Translation parameter, which is directly proportional to Time;

87  $n$  is the Normalising parameter and equal to 1 generally(say).

88 The variance of Wavelet coefficients follows power law relation with the scale which can be  
89 given by a simple equation given below;

$$90 \quad v = x^h$$

91 Here  $v$  is the variance of wavelet coefficients;  $x$  is the scale and  $h$  is the holder/wavelet  
92 exponent.

93 Holder/Wavelet exponent provides the measure of roughness/smoothness. If the holder  
94 exponent values are high, it accounts for smoothness whereas low values of holder exponent  
95 emphasis more roughness. After obtaining the holder exponent it can be substituted in the  
96 equation given below to obtain the fractal dimension Value;

$$97 \quad 2D = 5 - h$$

98 Here,  $D$  is the fractal dimension (FD).



99 **2.3 Discrete Wavelet Transform**

100 One- dimensional Discrete Wavelet Transform has been carried down in this task as per the  
101 datasets, which are discrete and one dimensional. For the construction of DWT one sets, a =  
102  $2^j$  and  $b = 2^j k$ , where  $j$  and  $k$  are both integers. 1-D DWT is given by the following equation,

103 
$$D_j(k) = 2^{-\frac{j}{2}} \int_{-\infty}^{\infty} f(t) \varphi(2^{-j}t - k) dt \quad (2)$$

104 Where  $f(t)$  is the time series of our interest;  $K=1, 2, 3, \dots, n$ ,  $n$  being the Discrete data array  
105 of maximum Size. Time series of our interest is decomposed to Approximate and Detailed  
106 Coefficients providing both lower and higher frequency information respectively.

107

108 **3.0 Results and Discussions**

109 **3.1 Application to Synthetic data**

110 A Synthetic signal is generated with three different frequencies such as 3Hz, 5Hz and 10Hz  
111 and analysed by CWT and also applied to synthetic signal added with 25% Gaussian white  
112 noise. The result obtained is shown in Figure 1. As the signal is free from noise possessing  
113 only its own frequencies the mathematical tools didn't posed any difficulty and the  
114 information required are derived without any ambiguity. When the same signal analyzed by  
115 the above mentioned techniques after mixing noise, it provides large difference in the results  
116 which are shown in Figure 2. The CWT provides an acceptable picture in analysing the non-  
117 stationary as well as the same non-stationary signal mixed with noise. CWT not only removes  
118 the ambiguity through by forming wavelet modulus maxima but also through its Wavelet  
119 Coefficients. Also it provides a picture of the Time-Frequency localisation in interpretable  
120 form. An advantage pertaining to wavelet transform is that the Wavelet coefficients records  
121 the exact information of the signal even it is noisy. This notion regarding CWT proves it as a  
122 good tool for identification of lithology in Well logs. Therefore, this technique can be used in  
123 all circumstances to derive the exact information in the Signal.



124 Mostly, Porosity logs are used for this approach and the fluctuating nature of the porosity  
125 logs can be correlated to both Pores distribution and the fracture (major as well as several  
126 micro fractures) as well. DWT differentiates both fractures and the characteristics of the  
127 pores in the detailed coefficients (Sahimi and Hashemi, 2001). Suppose, the datasets are  
128 collected in a fracture less well than the wavelet detail coefficient (WDC) plot will be  
129 featureless as given below (left of Figure3) but if the datasets are collected in a fractured well  
130 then the WDC plot will be containing highly differentiable features in terms of spikes or local  
131 maxima (right of Figure 3). Same log signal is used in the right one but certain data points are  
132 removed and replaced. The data points which do replaced pertaining to the uniform  
133 distribution constitute both low and high values in comparison with its surrounding data  
134 points. DWT differentiates these particular locations by means of a spike irrespective of the  
135 magnitude of the data points replaced. DWT exposes the signal to low and high frequency  
136 filters produces Detailed and Approximate coefficients respectively.

137

### 138 **3.2 Application of Field Data: Costa Rica Convergent Margin, Central America**

139 Costa Rica Convergent Margin in Central America is due to the convergence of Cocos and  
140 Caribbean Plates. A seismic migrated section over the region is shown in the Figure  
141 4showing Well sites 1039, 1040 and 1043. Among these wells sites 1039 and 1043 are taken  
142 for study whereas the site 1040 is omitted as it is not passing through certain major litho-  
143 units. Logs such as gamma ray and density are taken for study and the gamma ray signals  
144 exhibiting sharp spikes which are attributed to presence of interbedded ash layers. From the  
145 gamma ray log various lithology are identified and correlated with site adjacent to it. Density  
146 Logs are used for identification of spatial distribution of fractures along the rock matrix using  
147 DWT and WBFA. Core Analysis reports the presence of four sedimentary layers terminated  
148 by a concordant Igneous Intrusion Gabbroic Sill. Well site 1039 is taken as the reference and



149 lithology identified through Wavelet Transform are correlated to the site-1043 and the result  
150 confirms the subduction zone (Figure 7).

151 As conventional technique such as Fast Fourier Transform fails in providing the time-  
152 frequency localisation. So, the application of wavelet Transform is the only way to find the  
153 proper time-frequency localisation. The results obtained from CWT analyzed using log data  
154 sets prove the lithological successions. The stratigraphic interfaces occurring in the Well log-  
155 1039 (Figure 5) appears in the Well log-1043 (Figure 6) after having disruptions in the  
156 middle. From the seismic section it is seen that there are four major lithology running from  
157 the Well-1039 to Well-1043 and terminated as Gabbroic Sill. The Well-1040 crossed the  
158 above mentioned strata very mildly and it didn't reach the Concordant intrusive structure as  
159 reached by the Wells-1039 and 1043. Therefore, for interpretation point of view only the  
160 Wells-1039 and 1043 are used. The major successions mentioned after drilling is that the four  
161 sedimentary interfaces followed by a Gabbroic sill. The sedimentary succession obtained  
162 underneath the reference site-1039 situated in the Cocos Plate found to occur in the site-1043  
163 without any disruption. It is also noted from the observation made by Eric et al., (2000) as the  
164 Cocos Plate subducting under the Caribbean Plate the off scarping of the sediments in the  
165 Cocos Plate should occur on the overriding plate but on analysing the chemical composition  
166 it was mentioned the sediment lying on the overriding plate was of different composition.  
167 This analyses comes in support of the effort of framing the subducting system of Costa Rica  
168 using CWT shown in the Figure 7, it is observed that the sedimentary succession in the site-  
169 1039 over the subducting Cocos Plate continuing through the site-1043 without any  
170 disruption situated over the overriding Caribbean plate. In accordance to the locations of the  
171 Wells and the continuity of the sedimentary successions existing in the both sites (1039 and  
172 1043) as traced by the Wavelet scalogram, it is found that the Cocos Plate is subduction  
173 under the Caribbean plate. The lithology identified through time and frequency localisation



174 tools are used for the WBFA by taking their data points separately. Table 1 shows the FD  
175 values of various lithofacies of both well. From Table 1, we observe that there is transitional  
176 change between sandy and Shaly environments on the basis of variation in FD values and this  
177 variation corresponds to a gradual transition between different sedimentary environments.  
178 Hence, our study suggests that the FD can be used as a well log attribute or even a post-stack  
179 seismic attribute for reservoir characteristic (Brown, 2004).

180 In Table 1, FD values are greater than 1.2 that emphasises the presence of high shale  
181 content and of low energy environment in depth range between 210 and 330 and between 315  
182 and 430 as reported the presence of sandstone in well site 1039 and 1043 respectively (Figure  
183 10-11). In spite of the presence of sandstone the fractal dimension values are exceeding 1.2  
184 indicating the dominance of shale content and the values are found to be not consistent from  
185 reference site and site 1043. In prior depth ranges, the inconsistency of fractal dimension  
186 values are attributed to the presence of fractures from the structural observations obtained in  
187 well site but in the above mentioned depth ranges the inconsistency as well as from the holder  
188 exponent values it is noted that the roughness exists in the particular lithology. The analysed  
189 results are well correlated with the core samples.

190

## 191 **7. Conclusions**

192 Lithology identification is a tedious job in well logging and it is the most important one for  
193 reservoir characterisation. To identify Presence of structural feature such as fracture by quick  
194 look interpretation methods is very difficult using well log data. Formation micro imager  
195 (FMI) log often used to identify it is very expensive. Thus methodology used for lithology  
196 and fracture identification using wavelet transform and wavelet based fractal analysis using  
197 holder exponent can be a useful stuff to extract the different lithological feature as well as  
198 stratigraphy feature.



199 For structural feature identification from various lithologies holder exponent and  
200 fractal dimension values can be utilised and in the presence of some extra information as that  
201 of the structural observations from well sites the results can be more promising. In order to  
202 avoid the assistance of extra information more datasets are needed from the same area so that  
203 on application of WBFA on various lithologies passing through the area provides concrete  
204 idea on lithology and Structural features using holder exponent and fractal dimension values.

205

#### 206 **Acknowledgement**

207 The authors are grateful to editor and Associate editor for critical comments and useful  
208 suggestions to improve our manuscript for publication.

209

#### 210 **Figure and Table Captions**

211 Figure 1: Shows the Continuous Wavelet Transform (CWT) using a synthetic time series  
212 data.

213 Figure 2: Shows the Continuous Wavelet Transform (CWT) of a synthetic noisy time series  
214 data,

215 Figure 3: (a) Shows Discrete wavelet Transform (DWT) using synthetic data and original  
216 signal and its DWC-1 below it, (b) synthetic data and original signal edited at certain  
217 points and it's DWC-1 below it.

218 Figure 4: Shows the seismic migrated section showing the Wells (after Erik et al, 2000)

219 Figure 5: showing Continuous Wavelet Transform (CWT) using gamma ray signal and the  
220 Wavelet Coefficient at an altitude-32 of the gamma ray log of the Well location-1039

221 Figures 6: Showing Continuous Wavelet Transform (CWT) using gamma ray signal and the  
222 Wavelet Coefficient at an altitude-32 of the gamma ray signal of the Well location-

223 1043



224 Figure 7: Represents the lithology identification using the gamma ray log of the Well site  
225 1039 and 1043 by the lines drawn on the scalogram and it represents the subduction  
226 zone in the areas obtained from the seismic migrated section.

227 Figure 8: (a) Shows the discrete detailed and approximate coefficients and the spikes  
228 represents the possible fractures at well location 1039, (b) shows the Discrete detailed  
229 and Approximate coefficients and the spikes represents the possible fractures at well  
230 location 1043

231 Figure 9: shows the scale of interest shows variance of wavelet coefficients versus scale of  
232 gamma ray of well site 1039 and 1043

233 Figure 10: Shows variance of Wavelet coefficients versus scale of density log of well site-  
234 1039 and 1043 which shows consistent holder exponent and fractal dimension values  
235 indicating that wells contains similar sedimentary environment.

236 Figure 11: shows the FD values of both well sites of 1039 and 1043.

237 Table 1: Shows the FD values of the appropriate lithology identified and the circled depth  
238 ranging and its appropriate fractal dimension values showing deviation of the vales  
239 from the reference site 1039.

240 Table 2: Shows the ranges of fractal dimension values.

241

## 242 **References**

243 Brown, R. A.: Interpretation of three-dimensional seismic data, 6<sup>th</sup> edition, American  
244 Association of Petroleum Geologists (AAPG) Eds., 540pp., 2004.

245 Coconi-Morales E., Ronquillo-Jarillo G. and Campos-Enríquez J.O., Multi-scale analysis of  
246 welllogging data in petrophysical and stratigraphic correlation: Geofísica  
247 International, 2010, 49 (2), 55-67.



- 248 Chandrasekhar E., Rao E. V. Wavelet Analysis of geophysical welllog data of Bombay  
249 Offshore Basin, India, *Mathematical Geosciences*, 2012, 44, 901–928.
- 250 Dashtian, H., Jafari, Z., Lai, K., Sahimi M., Masihi, M., Analysis of cross correlation between  
251 well logs of hydrocarbon reservoirs. *Transp Porous Med*, 2011, 90, 445-464.
- 252 Daubechies, I., The wavelet transform time-frequency localization and signal analysis: *IEEE*  
253 *Transaction on Information Theory*, 1990, 36, No. 5.
- 254 Erik Moritz, Stefan Bornhold, Hildegard Westphal, Martin Meschede, Neural network  
255 interpretation of LWD data (ODP Leg 170) confirms complete sediment subduction at  
256 the Costa Rica convergent margin, *Earth and Planetary Science Letters*, 2000, 174,  
257 301-312.
- 258 Hui Liu and Zaixing Jian. Wavelet Transform of geophysical well logging signal and Its  
259 application to sequence division, 3<sup>rd</sup> International Congress on Image and Signal  
260 Processing, 2010, 3470-73.
- 261 J. F. Yu and Z. X. Li. Wavelet Transform of Logging Data and Its Geological Significance.  
262 *Journal of China University of Mining &Technology*, 2003, 32 (3): 336-339.
- 263 J. T. Li, J. F. Yu and Z. X. Li. The demarcating of Stratigraphic sequence based on wavelet  
264 Transform of well-logging data. *Coal Geology & Exploration*, 2004, 32 (3): 48-50.
- 265 Javid, M., and Tokhmechi, B. Formation interface detection using Gamma Ray log: A novel  
266 approach *Journal of Mining &Environment*, 2012, 3, 1, 41-50.
- 267 Mansinha, L., Stockwell, R. G., Lowe, R., Eramian, M., and Schincariol, R. A., Local S-  
268 spectrum analysis of 1-D and 2-D data, *Physics of the Earth &Planetary Interior*,  
269 1997,103, 329-336.
- 270 Pan, S., Hsieh, B., Lu, M. and Lin, Z., Identification of stratigraphic formation interfaces  
271 using wavelet and Fourier transforms: *Computers & Geosciences*,2008, **34**, 77–92.



- 272 Pinnegar, C. R. Mansinha, L., Time-local Fourier analysis with a scalable, phase-modulated  
273 analyzing function: TheS-transform with a complex window, *Signal Processing*, 2004,  
274 84, 1167-1176,
- 275 Pinnegar, C. R. Mansinha, L., The S-transform with window of arbitrary and varying shape,  
276 *Geophysics*, 2003, 68, 1, 381-385.
- 277 Pratt, W.K., *Digital Image Processing*, John Wiley & Sons, 1978, 330-333.
- 278 Sahimi, M., and Hashemi, M., 2001, Wavelet identification of the spatial distribution of  
279 fractures: *Geophysical Research Letter*, 28,4, 611–614.
- 280 Stockwell, R. G., Mansinha, L., and Lowe, R. P. Localization of complex spectrum: The S-  
281 Transform, *IEEE Transactions on Signal Processing* 1996, 144, 998–1001.
- 282 Stockwell R.G., Why use the S-Transform? *AMS Pseudo-differential operators: partial*  
283 *differential equations and time-frequency analysis*, 2007, 52, 279–309.
- 284 Tokhmechi, B., Memarian, H., Rasouli, V., Ahmadi N. H. and Moshiri, B. Fracture zones  
285 detection using wavelet decomposition of water saturation log. *J. Petrol. Sci.*  
286 *Eng.*, 2009a, 69, 129-138.
- 287 Tokhmechi, B., Memarian, H., Ahmadi N. H. and Moshiri, B., A novel approach for fracture  
288 Zone detection using petrophysical logs. *J. Geophys. Eng.*, 2009b, 6, 365-373.
- 289
- 290 Yue, W.Z., Tao, G., Liu, Z.W., Identifying reservoir fluids by wavelet transform of  
291 well logs. In: *Proceedings of the SPE Asia Pacific Oil and Gas Conference and*  
292 *Exhibition*, Perth, Australia, 2004, (SPE 88559).
- 293 Zhang Xiao-Feng, Pan Bao-Zhi, Wang Fei, and Han Xue, A study of wavelet transforms  
294 applied for fracture identification and fracture density evaluation, *Applied*  
295 *Geophysics*, 2011, 8, 2, 164-169.
- 296



297 Figure 1

298

299

300

301

302

303

304

305

306

307

308

309

310

311

312

313

314

315

316

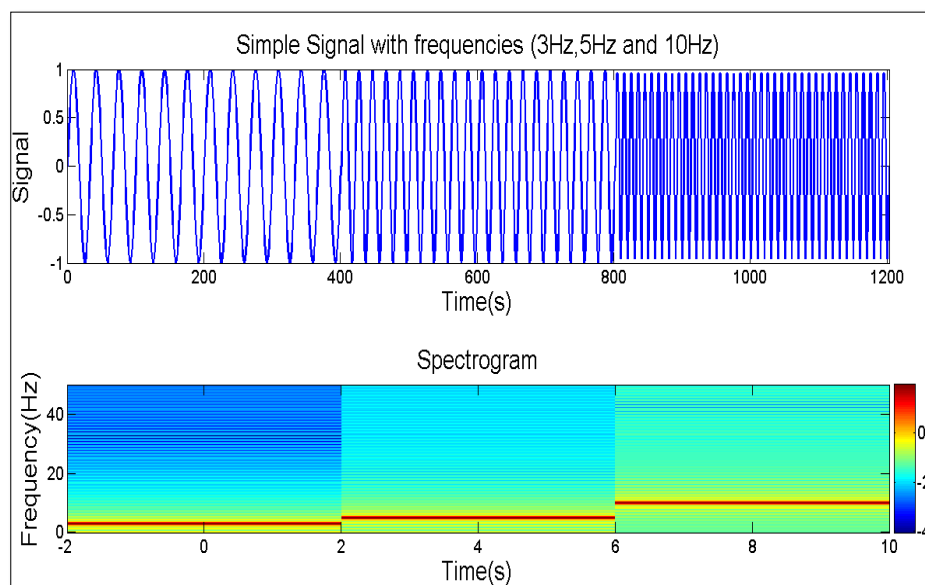
317

318

319

320

321





322 Figure 2

323

324

325

326

327

328

329

330

331

332

333

334

335

336

337

338

339

340

341

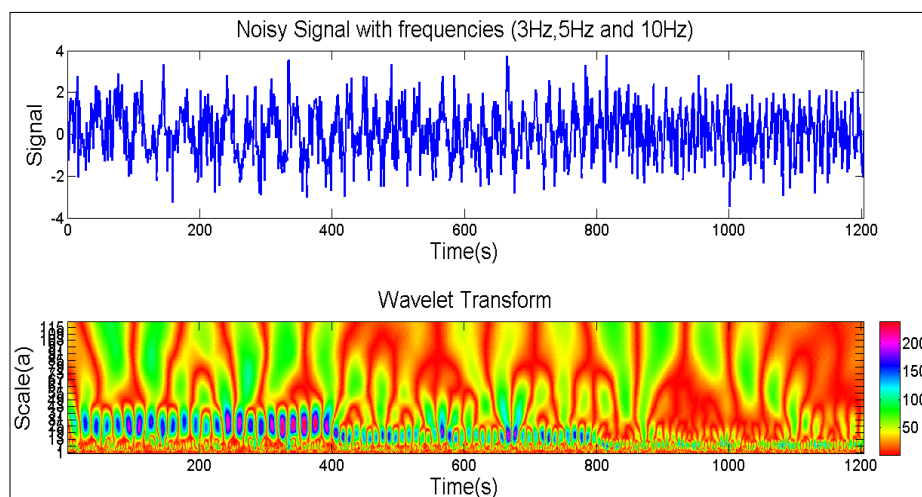
342

343

344

345

346





347 Figure 3(a)

348

349

350

351

352

353

354

355

356

357

358

359

360

361

362

363

364

365

366

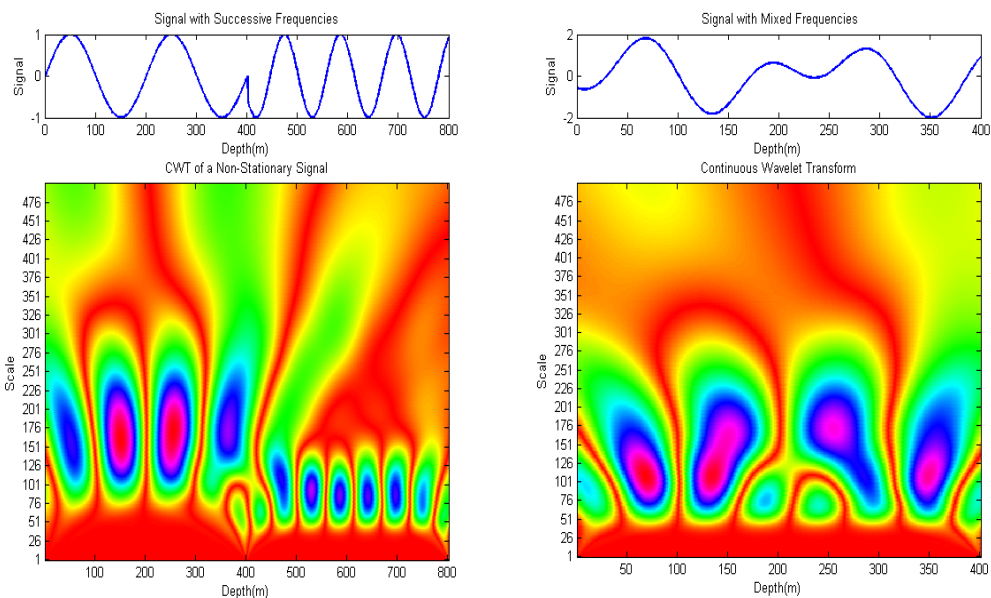
367

368

369

370

371





372 Figure 3(b)

373

374

375

376

377

378

379

380

381

382

383

384

385

386

387

388

389

390

391

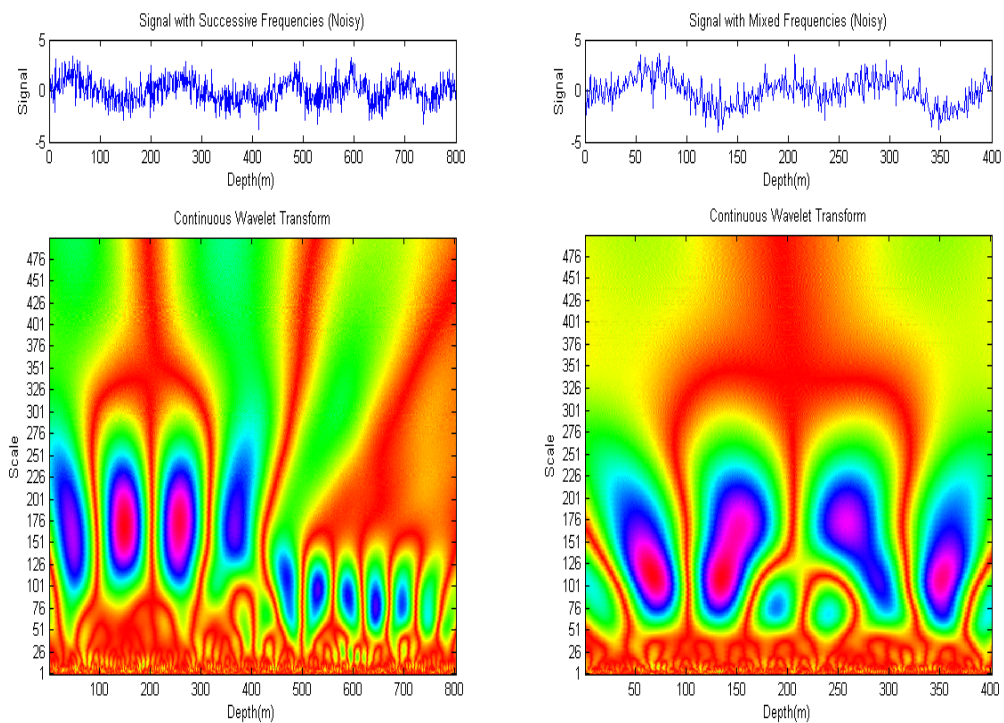
392

393

394

395

396





397 Figure 4

398

399

400

401

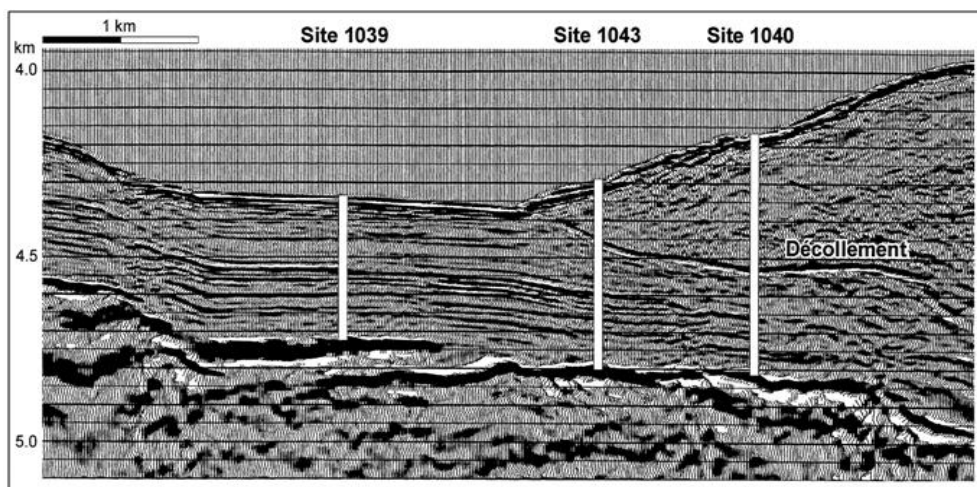
402

403

404

405

406



407

408

409

410

411

412

413

414

415

416

417

418

419

420

421



422 Figure 5

423

424

425

426

427

428

429

430

431

432

433

434

435

436

437

438

439

440

441

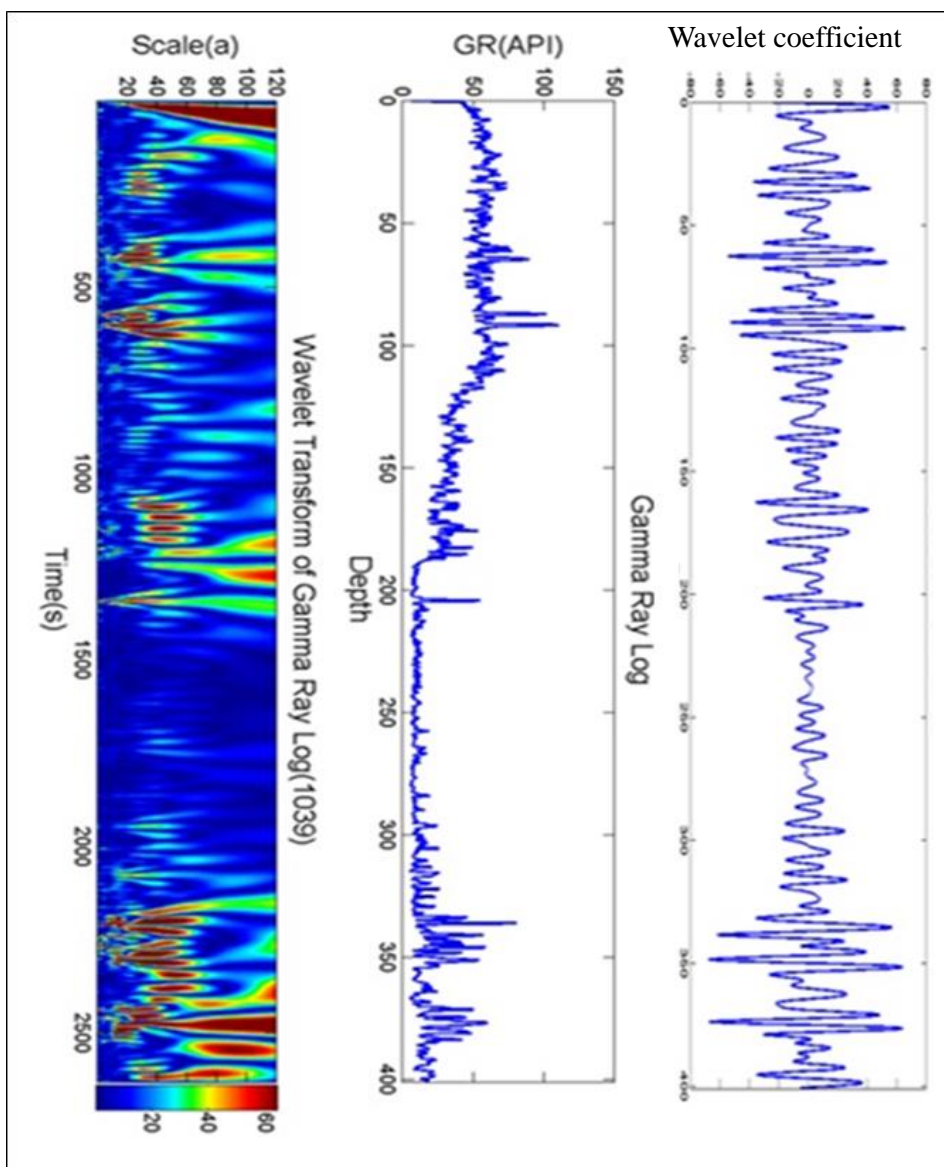
442

443

444

445

446





447 Figure 6

448

449

450

451

452

453

454

455

456

457

458

459

460

461

462

463

464

465

466

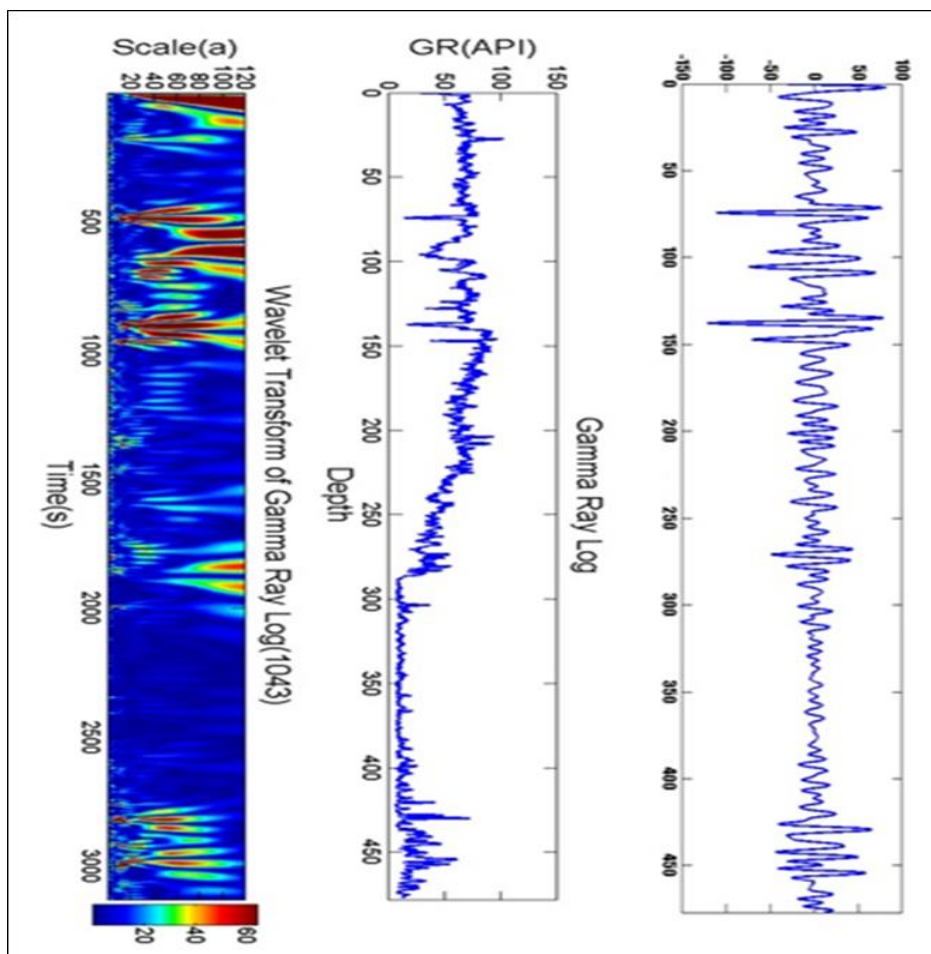
467

468

469

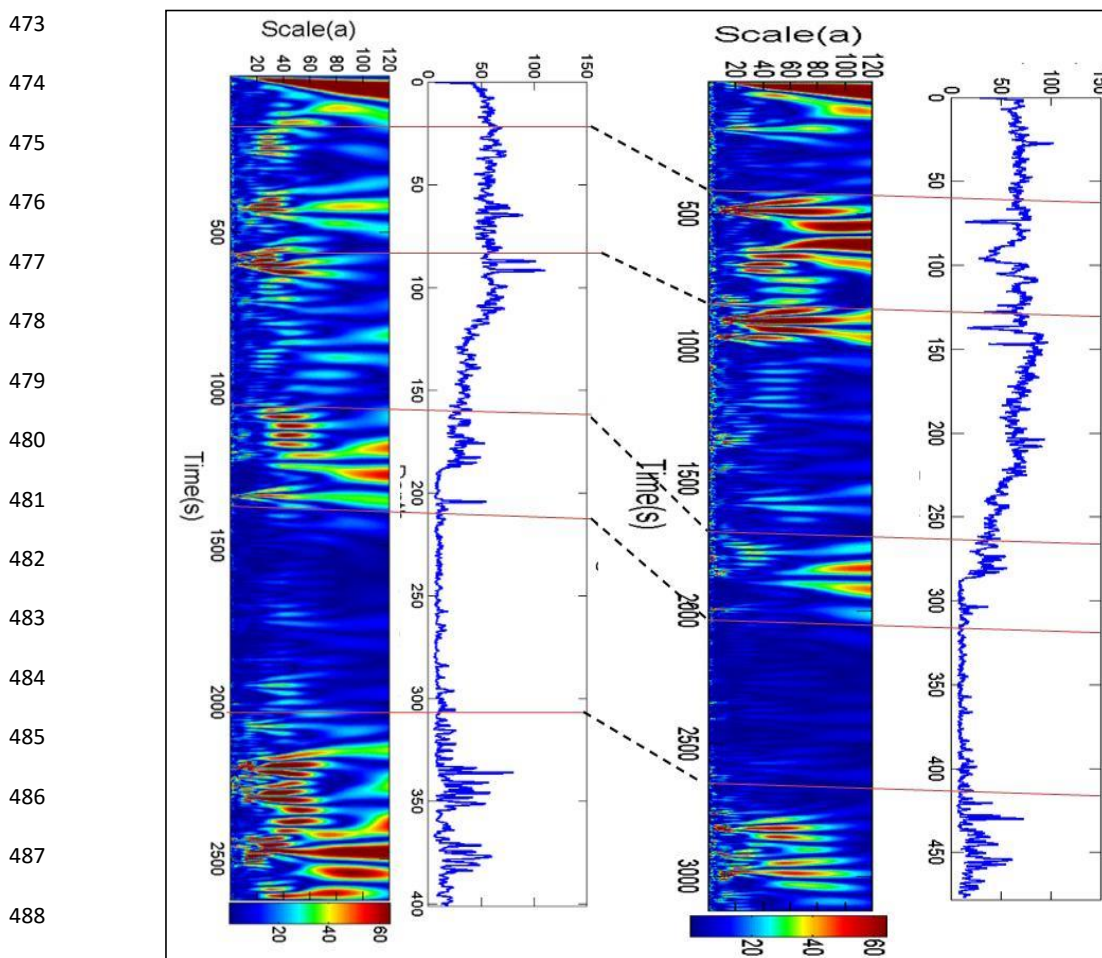
470

471





472 Figure 7





497 Figure 8

498

499

500

501

502

503

504

505

506

507

508

509

510

511

512

513

514

515

516

517

518

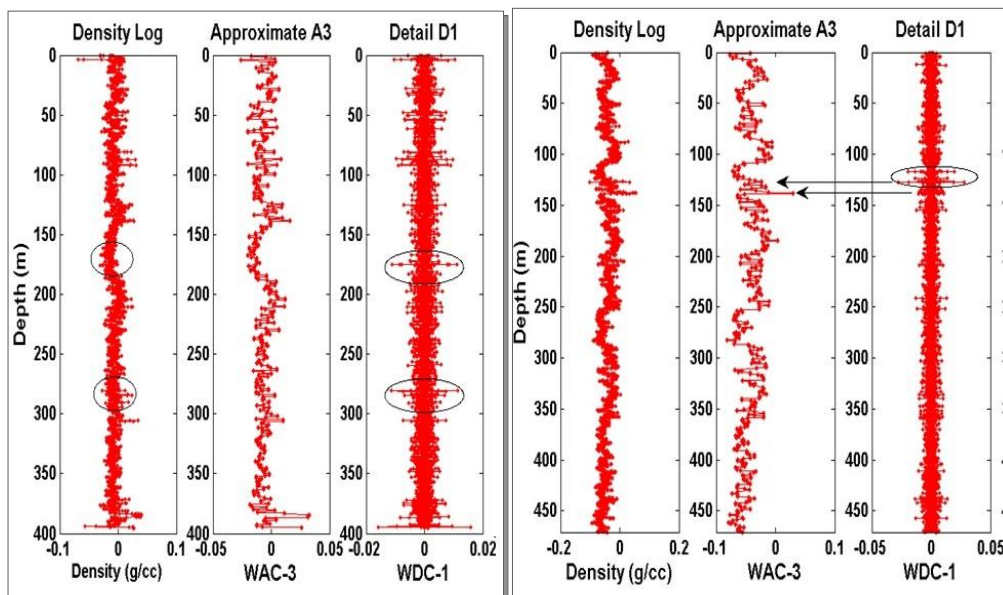
519

520

521

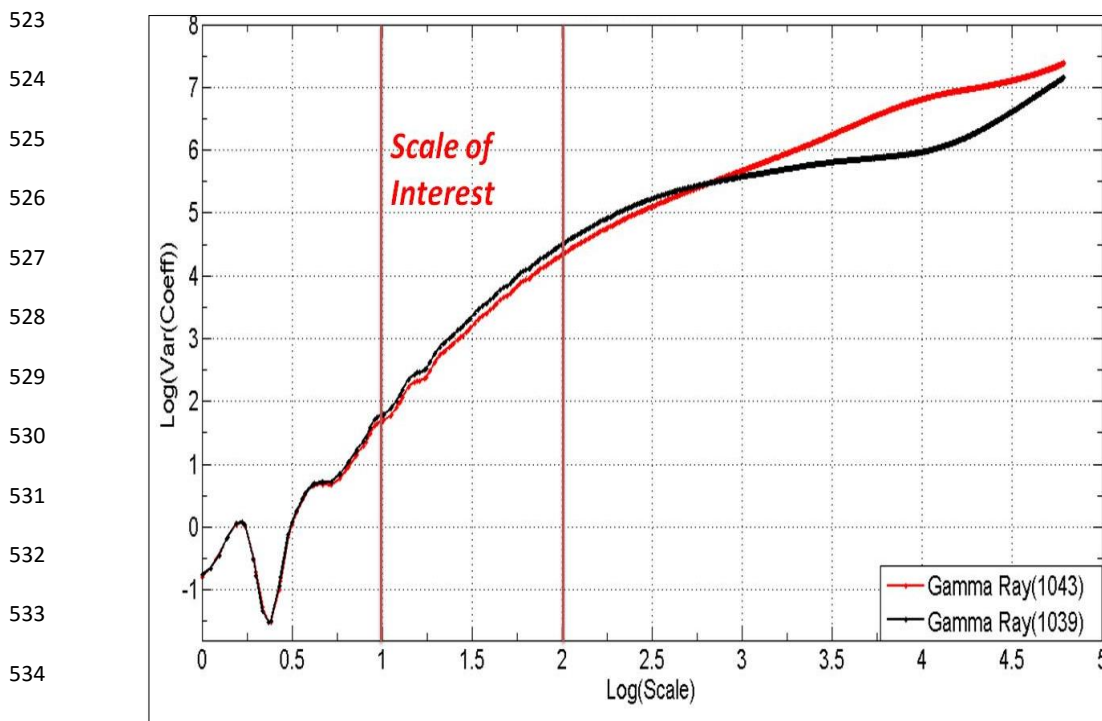
(a)

(b)



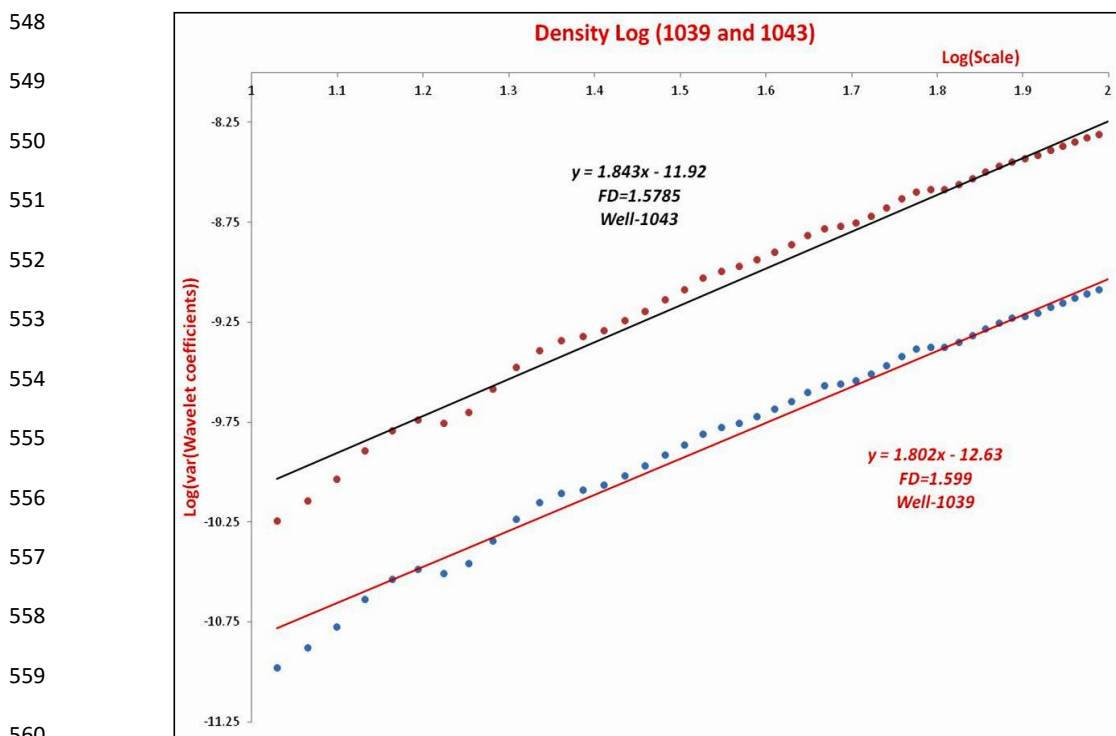


522 Figure 9





547 Figure 10



561

562

563

564

565

566

567

568

569

570

571



572 Figure 11

573

574

575

576

577

578

579

580

581

582

583

584

585

586

587

588

589

590

591

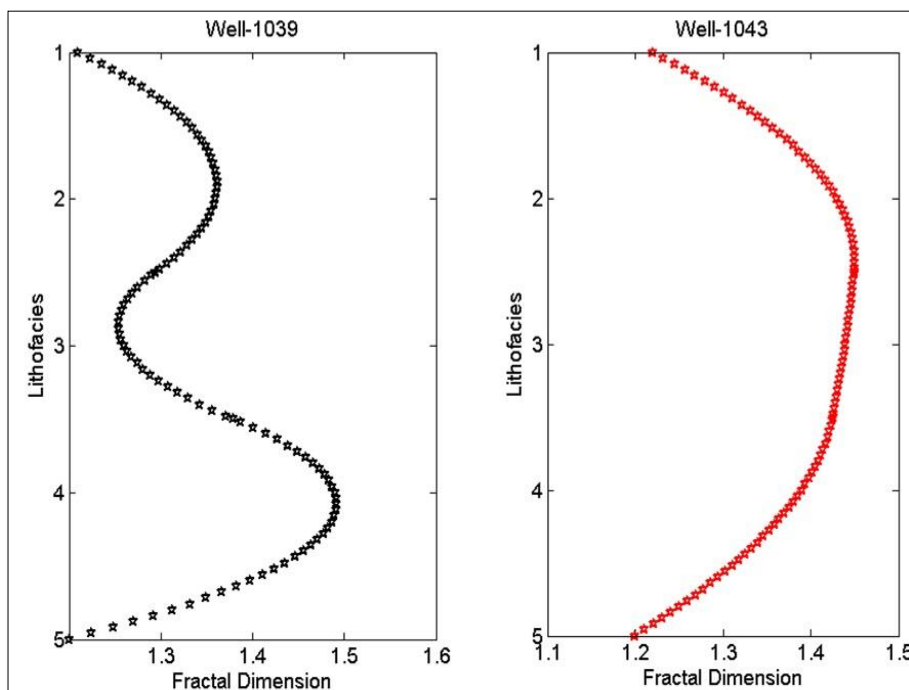
592

593

594

595

596





597 Table 1

598

599

600

601

602

603

604

605

606

607

608

609

610

611

612

613

614

615

616

617

618

619

620

621

Lithofacies	Depth range(meter)		Fractal Dimension	
	Well-1039	Well-1043	Well-1039	Well-1043
Shale with inter-bedded ash	20-80	60-130	1.21	1.22
Shaly sandstone	80-160	130-26	1.36	1.43
Sandy shale with inter-bedded ash	160-210	260-315	1.26	1.44
sandstone	210-330	315-430	1.49	1.39
Gabbroic Sill	330-400	430-450	1.20	1.20



622 Table 2

623

624

625

626

627

628

629

Fractal Dimension	Interpretation
< 0.9	High sand content and high energy environment
0.9 to 1.2	Inter-bedded sand and shale
> 1.2	High shale content and low energy environment